Performance–cost optimization of tuned mass damper under lowmoderate seismic actions

THE STRUCTURAL DESIGN OF TALL AND SPECIAL BUILDINGS
Struct. Design Tall Spec. Build. 2016;
Published online in Wiley Online Library (wileyonlinelibrary.com/journal/tal). DOI: 10.1002/tal.1300

Performance–cost optimization of tuned mass damper under low-moderate seismic actions

Rita Greco[1]*, Giuseppe Carlo Marano[2,3] and Alessandra Fiore[2]

[1]*DICATECH, Department of Civil Engineering, Environmental, Territory, Building and Chemical, Technical University of Bari, via Orabona 4, 70125 Bari, Italy*
[2]*DICAR, Department of civil Engineering and Architecture, Technical University of Bari, via Orabona 4, 70125 Bari, Italy*
[3]*College of Civil Engineering, Sustainable and Innovative Bridge Engineering Research Center (SIBERC), Fuzhou University, No2 Xue Yuan Road,University Town, Fuzhou, Fujian, China*

SUMMARY

In this paper, a multi-objective optimization of a single tuned mass damper is proposed at the aim to control vibrations induced in building structures under low-moderate earthquakes. The optimum design is carried out by considering both economic and performance criteria. The cost of the device is the economic objective that is assumed directly related to its mechanical parameters. At the aim to control the damage level and the behaviour of components and equipment, the ratio between the absolute accelerations of the protected structure and the unprotected one is assumed as the device performance. A multi-objective optimization is then formulated, and Pareto optimum solutions are achieved by the Non-dominated Sorting Genetic Algorithm in its second version. Finally, a sensitivity analysis of the optimum solution with respect to some input data is carried out. Copyright © 2016 John Wiley & Sons, Ltd.

Received 19 February 2016; Revised 13 April 2016; Accepted 18 May 2016

KEY WORDS: tuned mass damper; random vibrations; cost of protection system; multi-objective optimization; non-dominated sorting genetic algorithm

1. INTRODUCTION

The limitation of vibrations effects due to environmental dynamic loads is a very important matter in the design of civil and mechanical engineering structures. In this field, many different strategies have been proposed also with regard to safety structural problems induced by random vibrations action caused by natural or artificial loads, as for example earthquakes, wind pressure, traffic vibrations and sea waves. Generally, four groups of control systems are distinguished in literature: active, hybrid, semi-active and passive.

Among these, passive systems are the most unsophisticated and the cheapest ones. Passive systems have been used with success in many real cases: among the numerous existing passive control devices, the tuned mass damper (TMD) is frequently adopted both in mechanical systems and in civil structures, in new constructions as well as in retrofit interventions. In general, the purpose of installing a TMD is to guarantee a suitable level of protection in the primary structure in order to assure an adequate safety level, both for the structure and its contents, towards a defined limit state. Moreover, a TMD is introduced at the aim to reduce the discomfort of occupants and/or to limit the damage of equipments in particular in high-rise buildings (Marano and Greco, 2009) especially when low-moderate (and frequent) seismic loads are assumed in the design process. This last aspect is becoming extremely actual in civil engineering. Recent earthquakes have in fact shown that the damage in

*Correspondence to: Rita Greco, DICATECH, Department of Civil Engineering, Environmental, Territory, Building and Chemical, Technical University of Bari, via Orabona 4 - 70125 Bari, Italy.
E-mail: rita.greco@poliba.it

equipments and in building contents can have large economic consequences. For instance, in high-rise buildings, a localized damage in several acceleration-sensitive non-structural systems (suspend ceilings, light fixture, fire suppression piping systems, computer systems, emergency power generation systems, elevators, etc.) can affect the functionality of large portions of the building. Therefore, structural seismic design should be applied not only in order to guarantee the life safety and to prevent structural collapse but also in order to control the damage level and the behaviour of components and systems.

A TMD, placed at the top of a structure, is designed to dissipate energy in a purely mechanical way. The device is attached to the structure by a spring and a damper, in such a way that it oscillates at the same frequency of the structure, but with a shift of phase. The main mechanism of reducing the detrimental oscillations of the structure is achieved by transferring its vibration energy to the TMD, so dissipating the energy through the damping of the TMD.

With the purpose of maximizing TMD efficiency, over the years, numerous approaches have been proposed for the optimum design of TMD. After the work of Ormondroyd and Den Hartog (1928), several optimum design methods have been introduced in literature, aimed at minimizing the vibrations induced in mechanical and structural systems by various types of excitation sources (Crandall and Mark, 1973; Sadek *et al*., 1997; Rana and Soong, 1998; Hoang and Warnitchai, 2005; Rundinger, 2006; Hoang *et al*., 2008; Krenk and Høgsberg, 2008; Marano *et al*., 2010; Marano and Greco, 2011; Greco and Marano, 2013). In most of the above studies, the main structure is generally represented by an equivalent single degree of freedom system. Similarly, the performance of a TMD applied to a multi degree of freedom (MDOF) structure and optimized to control only a single mode of vibration (usually the fundamental one) has been investigated by various authors (Villaverde, 1985; Villaverde and Koyama, 1993; Sadek *et al*., 1997). The optimal parameters of single and multiple TMDs for the control of MDOF structures have been studied by several researchers in the last decades (Kareem and Kline, 1995; Zuo and Nayfeh, 2005; Zuo and Nayfeh, 2006; Li and Ni, 2007; San Mateo *et al*., 2011; Marano *et al*., 2013; Mohebbi *et al*., 2013) also considering the uncertainties affecting structural parameters (Greco *et al*., 2014a; Lucchini *et al*., 2014).

The above studies mainly take as objective function (OF) the efficiency of the TMD expressed by a performance index (PI) that generally is chosen as the ratio between the response (displacement, acceleration dissipated energy) of the unprotected system and the same quantity of the protected one.

However, although in recent years considerable efforts have been devoted to the mitigation of earthquake/wind-induced motions in the field of structural optimization, implementations of TMD vibration control technology on actual building design are limited. To a certain extent, impediments to the application of these techniques are attributable to the preconception on the associated high capital and on the long-standing maintenance costs of the auxiliary damping devices, due to the absence of a comprehensive cost analysis in the optimum design process.

In effect, often, especially for new and notably important buildings or in the case of retrofitting of existing constructions, the containment of costs is one of the most important target in the design of the protection system. Therefore, the individualization of a reliable and representative cost function and its introduction in the optimum design is a very important issue, especially in order to not only compare the effectiveness of systems in terms of performance but also verify the economic gain achieved through a particular design strategy rather than another one.

Differently from previous studies in this field, in this paper, an optimum design of a single TMD installed on the top floor of a structure modelled by a linear MDOF system is carried out at the aim to simultaneously minimize the protection system cost and maximize a direct index of performance of the TDM. Therefore, both a cost function and a PI are introduced in the optimum design strategy of the TMD. A multi-objective problem is so formulated, since there are two conflicting OFs: the PI and the cost of the device. In this context, the standard optimization approach, in which the optimum solution coincides with the minimum or the maximum value of a scalar OF, is inapplicable, and therefore Pareto optimum solutions (Zitzler and Thiele, 1999) are obtained. At this aim, the Non-dominated Sorting Genetic Algorithm II—NSGA-II—is adopted (Deb *et al*., 2000).

Moreover, the study is developed in a stochastic way, by introducing a Gaussian non-stationary filtered stochastic process to model the ground motion at the base of the structure. An extensive sensitivity analysis of the optimum solution in function of some input data is finally carried out.

2. ANALYTICAL FORMULATION OF THE TUNED MASS DAMPER PROBLEM FOR MULTI DEGREE OF FREEDOM SYSTEMS SUBJECTED TO RANDOM LOADS

A TMD can be modelled as a mass–dashpot–spring system (the secondary system) attached generally at the top of a MDOF oscillator (which represents the primary system), aimed at reducing in this one the detrimental vibrations induced by seismic actions. In engineering applications, the oscillator could be a building, a bridge, an offshore platform or mechanical equipment located on a vibrating support, and the use of a TMD would be intended to reduce the induced undesirable vibrations.

In this study, the problem of a single TMD positioned at the top of a main structure modelled as a linear viscous elastic MDOF system is analysed. Even if for high values of the displacement the structure may experience inelastic deformations that may induce inelastic nonlinear response (Fiore and Monaco, 2010; Fiore and Monaco, 2011; Fiore *et al*., 2013), the assumption of linear behaviour is quite accurate, since the TMD is designed to minimize the response, so avoiding large displacements.

A deterministic second-order mechanical linear system with $n+1$ degree of freedom is herein considered and described by using lumped masses, as shown in Figure 1. Under the hypothesis of random dynamic inputs, the dynamic system of motion can be written as

$$\mathbf{M}\ddot{\mathbf{X}} + \mathbf{K}\mathbf{X} + \mathbf{C}\dot{\mathbf{X}} = -\mathbf{M}\mathbf{r}\ddot{X}_b, \qquad (1)$$

where **M**, **C** and **K** are, respectively, the deterministic mass, damping and stiffness matrices (as detailed in appendix); $\mathbf{X} = (x_1, x_2, ..., x_n, x_T)^T$, $\dot{\mathbf{X}} = (\dot{x}_1, \dot{x}_2, ..., \dot{x}_n, \dot{x}_T)^T$ and $\ddot{\mathbf{X}} = (\ddot{x}_1, \ddot{x}_2, ..., \ddot{x}_n, \ddot{x}_T)^T$ are the tuned-structure relative displacement, velocity and acceleration vectors referred to each degree

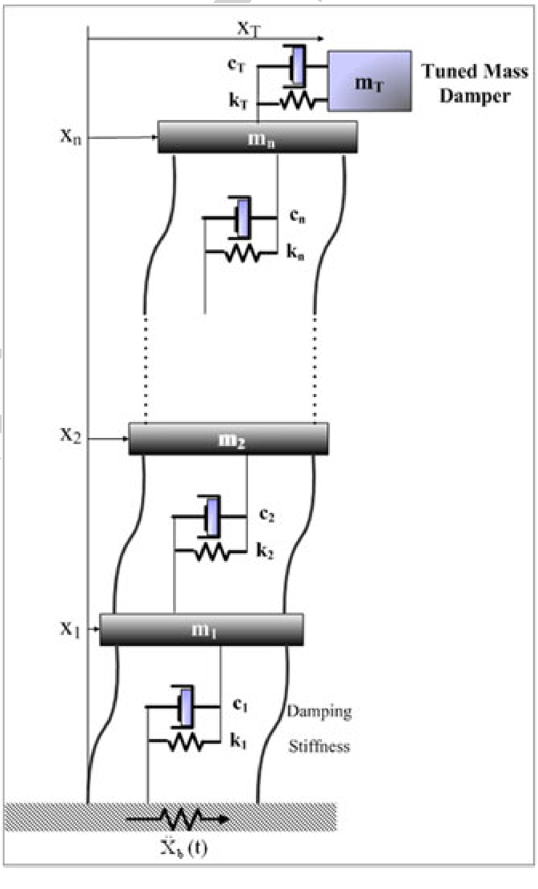

Figure 1. Multi degree of freedom system equipped with a tuned mass damper.

DOI: 10.1002/tal

of freedom; $\mathbf{r} = (1 \ldots, 1)^T$; $\ddot{X}_b(t)$ is the seismic action and, since it is mathematically described by a stochastic process, many advantages can be reached by modelling it through a *filtered white noise*.

For base random accelerations modelling, a wide adopted model in both stationary and non-stationary cases is those obtained by a simple linear second-order filtering of a white noise process. It is able to characterize input frequency modulation for a wide range of practical situations, and in case of non-stationary input, it is able to model not only amplitude but also time variation of frequency contents. In this study, the non-stationary Kanai Tajimi process is used to model the seismic action $\ddot{X}_b(t)$:

$$\ddot{X}_b = \ddot{X}_f + w\mathrm{V}(t) = -\left(2\xi_f\omega_f\dot{X}_f + \omega_f^2 X_f\right) \tag{2}$$

so that the filter acceleration is

$$\ddot{X}_f = -\omega_f^2 X_f - 2\xi_f\omega_f\dot{X}_f - wV(t), \tag{3}$$

where w is the stationary Gaussian zero mean white noise process with intensity S_0, supposed generated at the bed rock; ω_f is the filter frequency, given by

$$\omega_f = \sqrt{\frac{k_f}{m_f}}; \tag{4}$$

ξ_f is the filter damping, given by

$$\xi_f = \frac{c_f}{2\sqrt{m_f k_f}}. \tag{5}$$

The Jennings modulation function $V(t)$ (Jennings *et al*., 1968; Greco *et al*., 2014b) is adopted in this study. Then, the filter-structure system of Eq. (1) can be rewritten as

$$\ddot{\mathbf{X}} = -\left[\mathbf{M}^{-1}\mathbf{K}\right]\mathbf{X} + \left[\mathbf{M}^{-1}\mathbf{C}\right]\dot{\mathbf{X}} + \mathbf{r}\left(\omega_f^2\right)X_f + \mathbf{r}\left(2\xi_f\omega_f\right)\dot{X}_f \tag{6}$$

By introducing the *space state vector*, defined as follows:

$$\mathbf{Z} = \begin{bmatrix} \mathbf{X} \\ X_f \\ \dot{\mathbf{X}} \\ \dot{X}_f \end{bmatrix}, \tag{7}$$

Eq. (6) can be rewritten in the state space as

$$\dot{\mathbf{Z}} = \mathbf{AZ} + \mathbf{F} \tag{8}$$

In the above expression, the state system matrix $\mathbf{A}$ has the following form:

$$\mathbf{A} = \left[\begin{array}{c:c} 0^{(n+2)(n+2)} & \mathrm{I}^{(n+2)(n+2)} \\ \hdashline -\mathrm{H}_K & -\mathrm{H}_C \end{array}\right] \tag{9}$$

the two submatrices $\mathbf{H}_K$ and $\mathbf{H}_C$ are, respectively, given by

$$\mathbf{H}_K = \left[\begin{array}{c:c} & \omega_f^2 \\ & \omega_f^2 \\ (\mathbf{M}^{-1}\mathbf{K})^{(n+1)(n+1)} & \ldots \\ & \omega_f^2 \\ \hdashline 0 \quad .. \quad .. \quad 0 & -\omega_f^2 \end{array}\right] \tag{10}$$

DOI: 10.1002/tal

$$\mathbf{H}_C = \left[\begin{array}{c:c} & 2\xi_f\omega_f \\ (\mathbf{M}^{-1}\mathbf{C})^{(n+1)(n+1)} & 2\xi_f\omega_f \\ & \dots \\ & 2\xi_f\omega_f \\ \hdashline 0 \quad .. \quad .. \quad 0 & -2\xi_f\omega_f \end{array}\right] \tag{11}$$

The following vectors are then introduced:

$$\overline{\mu} = \left[\frac{m_2}{m_1} \dots \quad \dots \quad \frac{m_T}{m_n}\right] \tag{12}$$

$$\overline{\beta} = \left[\sqrt{\frac{k_1}{m_1}} \dots \quad \dots \quad \sqrt{\frac{k_T}{m_T}}\right] \tag{13}$$

$$\overline{\psi} = \left[\frac{c_1}{2\sqrt{k_1 m_1}} \dots \quad \dots \quad \frac{c_T}{2\sqrt{k_T m_T}}\right] \tag{14}$$

where m_T, k_T and c_T are the mass, the stiffness and the damping of the TMD, respectively.

The two submatrices $\mathbf{M}^{-1}\mathbf{C}$ and $\mathbf{M}^{-1}\mathbf{K}$ are given in Appendix 1.

Under the assumption that the system, in this form, is linear and that the input function is a Gaussian zero mean process, the response is a Gaussian zero mean process too. It follows that the knowledge of the covariance matrix $\mathbf{R_{ZZ}}$ allows to completely defining the space state of the statistic response. Then the probabilistic analysis is performed by solving the following non-stationary Lyapunov matrix differential equation (Marano *et al.*, 2015):

$$\dot{\boldsymbol{R}}_{ZZ} = \boldsymbol{A}\boldsymbol{R}_{ZZ} + \boldsymbol{R}_{ZZ}\boldsymbol{A}^T + \boldsymbol{B} \tag{15}$$

The matrix $\mathbf{B}$ has all null elements except one:

$$[\mathbf{B}]_{n+1,n+1} = 2\pi S_0 V^2(t) \tag{16}$$

Eq. (15) allows to determine the covariance matrix and finally to solve the motion equations.

The covariance matrix $\mathbf{R_{ZZ}}$ can be represented as

$$\mathbf{R_{ZZ}} = \begin{bmatrix} \mathbf{R_{XX}} & \mathbf{R_{X\dot{X}}} \\ \mathbf{R_{\dot{X}X}} & \mathbf{R_{\dot{X}\dot{X}}} \end{bmatrix} \tag{17}$$

$\mathbf{R_{XX}}$, $\mathbf{R_{X\dot{X}}}$, $\mathbf{R_{\dot{X}X}}$ and $\mathbf{R_{\dot{X}\dot{X}}}$ being the submatrices of $\mathbf{R}_{ZZ}$.

The absolute acceleration covariance matrix $\mathbf{R_{\ddot{y}\ddot{y}}} = \langle \ddot{\mathbf{Y}}\ddot{\mathbf{Y}}^{\mathrm{T}} \rangle$ is linearly related to the covariance matrix $\mathbf{R_{ZZ}}$ as follows:

$$\ddot{\mathbf{X}} = -\mathbf{H}_{\mathrm{K}}\mathbf{X} + \mathbf{H}_{\mathrm{C}}\dot{\mathbf{X}} + \mathbf{r}\ddot{X}_b, \tag{18}$$

$$\ddot{\mathbf{Y}} = \left(\ddot{\mathbf{X}} + \mathbf{r}X_b\right) = -\mathbf{H}_{\mathrm{K}}\mathbf{X} + \mathbf{H}_{\mathrm{C}}\dot{\mathbf{X}}, \tag{19}$$

$\ddot{\mathbf{Y}}$ representing the absolute acceleration of the system.

$$\mathbf{A} = \left[\begin{array}{c:c} 0^{(n+2)(n+2)} & \mathrm{I}^{(n+2)(n+2)} \\ \hdashline -\mathrm{H}_{\mathrm{K}} & -\mathrm{H}_{\mathrm{C}} \end{array}\right]$$

By introducing the unprotected system state vectors $\mathbf{U} = \left(\mathbf{X}_0 \ , \dot{\mathbf{X}}_0\right)^T$ and $\mathbf{D} = \left[\mathbf{H}_{\mathrm{K}} \quad \mathbf{H}_{\mathrm{C}}\right]$,where

$$\mathbf{X}_0 = (x_1, x_2, \ ...., x_n)^T, \ \ \dot{\mathbf{X}}_0 = (\dot{x}_1, \dot{x}_2, \ ...., \dot{x}_n)^T, \tag{20}$$

Eq. (19) can be rewritten as

DOI: 10.1002/tal

$$\ddot{\mathbf{Y}} = \mathbf{DU} \tag{21}$$

So the acceleration covariance matrix can be related to the system state covariance matrix $\mathbf{R}_{\mathbf{UU}} = \langle \mathbf{UU}^{\mathrm{T}} \rangle$ by the expression

$$\mathbf{R}_{\ddot{\mathbf{y}}\ddot{\mathbf{y}}} = \mathbf{D}\mathbf{R}_{\mathbf{UU}}\mathbf{D}^T. \tag{22}$$

3. MULTI-OBJECTIVE CRITERIA FOR TUNED MASS DAMPER MECHANICAL PARAMETERS

Standard optimization problem finds the optimum solution that coincides with the minimum or the maximum value of a scalar OF. The first problem definition of structural optimization was proposed by Nigam (1972), in which constraints were defined by using probabilistic indices of the structural response and the OF was defined by the structural weight. This led to a standard nonlinear constrained problem. However, the standard optimization problem does not usually hold correctly many real structural problems, where often different and conflicting objectives may exist. In these situations, the standard optimization problem is utilized by selecting a single objective and then incorporating the other objectives as constraints.

The main disadvantage of this approach is that it limits the choices available to the designer. This makes the optimization process a difficult task. Instead of unique standard optimization problem solution with a single given constraint, a set of alternative solutions can be usually achieved, known as Pareto optimum solutions. These represent the best solutions in a wide sense that means they are superior to other solutions in the search space, when all objectives are considered. If any other information about the choice or preference is given, no one of the corresponding trade-offs can be said to be better than the others.

In this section, a multi-objective optimization of a TMD installed on a MDOF system is formulated as the search of a suitable set of design variables, collected in the so called design vector (DV) $\mathbf{b} \in \mathbf{\Omega}_{\mathbf{b}}$, $\mathbf{\Omega}_{\mathbf{b}}$ being the admissible domain, which minimize two OFs.

With regard to the selection of design variables, one should point out that in the optimum design of TMD, it is common to consider only the TMD frequency and damping ratio as design variables (ref). The TMD mass or the ratio μ between the main system mass and the TMD mass is usually assumed as a constant parameter, which is defined in a pre-design stage (Marano *et al*., 2010). In this study, the authors analyse two cases: a two dimension DV $\mathbf{b} = (\omega_T, \xi_T)$ and a complete design, which assumes in the DV $\mathbf{b} = (\omega_T, \xi_T, \mu)$ also the mass ratio.

Concerning the selection of the OFs, the effectiveness of a seismic control device, such as a TMD, is usually measured in terms a PI that is selected to adequately estimate the reduction of seismic demand in the protected structure. The optimum properties of the TMD are those corresponding to a minimum or maximum value of the PI. Different performance indices can be used to evaluate the effectiveness of a control strategy, and based on the selected index, different solutions can be obtained. The PI may be defined in terms of floor accelerations, story drifts, base shear and other response quantities of interest. In this study, the acceleration is used as a measure of damages of non-structural components.

The first OF to be minimized is therefore the ratio between the standard deviation of the top floor absolute acceleration of the protected structure $\sigma_{\ddot{y}_N}$ and the one of the unprotected structure $\sigma^0{}_{\ddot{y}_N}$:

$$OF_1 = I_{\ddot{y}_N} = \frac{\sigma_{\ddot{y}_N}(\mathbf{b})}{\sigma^0{}_{\ddot{y}_N}} \tag{23}$$

This function represents a direct stochastic index of vibration protection effectiveness, coherently with the strategy to reduce those structural detrimental vibrations that can induce damages in contents and equipment, as required in operational performance level. This parameter shows protection effectiveness when its value is smaller than one. At the same time, a value of the OF close to the unit indicates practically negligible effects in vibration control (greater values are for negative TMD effects, increasing structure acceleration).

DOI: 10.1002/tal

The second objective is to minimize the *cost* related to the use of a TMD system. Frequently, especially for new and notably important buildings or for retrofitting of existing constructions, the containment of costs is one of the most important targets in a protection system design. Therefore, the individualization of a reliable and representative cost function is very important, especially in order to not only compare the effectiveness of systems in terms of performance but also verify the economic gain achieved in a particular design strategy rather than another. For this purpose, first of all, it is necessary to define the meaningful cost components. For a TMD protection strategy, the greatest portion of the installation cost is related to the mechanical characteristics of the system. Moreover, other cost parameters should be considered (for instance, control and maintenance costs), but the impact of sensors, computer control systems and future regulations in passive devices is drastically reduced (and practically negligible) in comparison with active or hybrid ones. Therefore, in this paper, only the cost associated with the mechanical characteristics is considered.

Two different situations are herein analysed.

a) As a first case, it is assumed that the mass ratio μ is a fixed quantity; therefore, for each possible DV, in this context defined as

$$\mathbf{b} = (\omega_T, \xi_T)^T \tag{24}$$

without loss of generality, it is assumed that the cost of the TMD is expressed as a linear function of the mechanical design parameters k_T and $c_{T,}$ respectively, so that

$$C_T^1 = k_T + \alpha_C c_T \tag{25}$$

where α_C is the cost parameter. Moreover, by considering that the damping device has in general a different (higher) unit cost in comparison with the stiffness one, the cost parameter α_C is defined as the ratio between these two unitary costs:

$$\alpha_C = \frac{\text{cost}(c_T = 1)}{\text{cost}(k_T = 1)} \tag{26}$$

Introducing in Eq. (25) the terms: $k_T = \omega_T^2 m_T$, $\mu = m_T/m_S$ and $c_T = 2\xi_T\omega_T m_T$, Eq. (25) can rearranged as below:

$$C_T^1(\mathbf{b}) = \mu m_S\left[\omega_T^2 + 2\alpha_C\xi_T\omega_T\right] \tag{27}$$

The protection system cost for a unit system mass m_S, finally, is given by

$$OF_2 = I_{C_T^1}(\mathbf{b}) = \frac{C_T^1(\mathbf{b})}{m_S} = \mu\left[\omega_T^2 + 2\alpha_C\xi_T\omega_T\right] \tag{28}$$

b) As a further design case, also the mass ratio μ can be assumed as a design variable. Therefore, by assuming that the structural mass m_S is known, the mass of the TMD m_T is the new variable introduced in the evaluation of the cost of the protection system. The cost of a TMD in this situation depends on k_T, c_T, m_T and the new DV $\mathbf{b}$ as follows:

$$C_T^2(\mathbf{b}) = k_T + \alpha_C c_T + \theta_T m_T \tag{29}$$

where $\mathbf{b}$ can be expressed as

$$\mathbf{b} = (\omega_T, \xi_T, \mu)^T \tag{30}$$

while θ_T is a new cost parameter defined as

$$\theta_T = \frac{\text{cost}(m_T = 1)}{\text{cost}(k_T = 1)} \tag{31}$$

In the same way, as previously explained, relation Eq. (29) can be reorganized as

$$C_T^2(\mathbf{b}) = \mu m_S\left[\omega_T^2 + 2\alpha_C\xi_T\omega_T + \theta_T\right] \tag{32}$$

The protection system cost for a unit mass m_S finally is given by

DOI: 10.1002/tal

$$OF_2 = I_{C_T^2}(\overline{b}) = \frac{C_T^2(\overline{b})}{m_S} = \mu\left[\omega_T^2 + 2\alpha_C\xi_T\omega_T + \theta_T\right] \quad (33)$$

Finally, the following multi-objective optimum design problems are formulated:a) Find

$$\mathbf{b} = (\omega_T, \xi_T)^T \quad (34)$$

that minimizes $OF_1,\ OF_2$;b) Find

$$\mathbf{b} = (\omega_T, \xi_T, \mu)^T \quad (35)$$

that minimizes $OF_1,\ OF_2$.

In the case of conflicting objectives, such as the analysed case, it is not possible to obtain a single optimum solution but rather a set of alternative solutions. These are the best possible solutions meaning that it is impossible to make any of the OFs better off without making the other worse off. These solutions, in accordance with the definitions and principles of Pareto dominance and Pareto optimality (Srinivas and Deb, 1994), are usually called Pareto optimum solutions. The Pareto optimal solutions can be identified using Evolutionary Multi-objective Optimization algorithms (Fiore *et al*., 2012; Quaranta *et al*., 2014; Fiore *et al*., 2015). One of them is the Strength Pareto Evolutionary algorithm, which is based on the theory of Evolution Strategies. Its most important feature is that it preserves the diversity in the population, so that a well-distributed widespread trade-off front is obtained by preventing premature convergence to a specific part of the Pareto front. In addition, it uses clustering in order to reduce the number of non-dominated solutions representing the whole Pareto front. In alternative, the NSGA (Srinivas and Deb, 1994) could be adopted.

4. AN OVERVIEW ON MULTI-OBJECTIVE OPTIMIZATION USING GENETIC ALGORITHM

Many real engineering problems often involve several OFs, each other in conflict. In these situations, it is not possible to define a universally approved criterion of 'optimum' as in single objective optimization. Instead of aiming to find a single solution, one can try to produce a set of good compromises. In a typical multi-objective optimization by genetic algorithm minimization-based multi-objectives optimization (MOOP), given two candidate solutions $\{\mathbf{b}_j, \mathbf{b}_k\}$, if

$$\forall i \in \{1, \ldots, M\}, OF_i(\mathbf{b}_j) \leq OF_i(\mathbf{b}_k) \wedge \exists i \in \{1, \ldots, M\} : OF_i(\mathbf{b}_j) < OF_i(\mathbf{b}_k) \quad (36)$$

and defined the two objective vectors

$$\mathbf{v}(\mathbf{b}_j) = \{OF_1(\mathbf{b}_j), \ldots, OF_M(\mathbf{b}_j)\} \quad (37)$$

$$\mathbf{v}(\mathbf{b}_k) = \{OF_1(\mathbf{b}_k), \ldots, OF_M(\mathbf{b}_k)\}, \quad (38)$$

the vector $\mathbf{v}(\mathbf{b}_j)$ is said to dominate vector $\mathbf{v}(\mathbf{b}_k)$ (denoted by $\mathbf{v}(\mathbf{b}_j) \prec \mathbf{v}(\mathbf{b}_k)$).

Moreover, if no feasible solution, $\mathbf{v}(\mathbf{b}_k)$, exists that dominates solution $\mathbf{v}(\mathbf{b}_j)$, then $\mathbf{v}(\mathbf{b}_j)$ is classified as a non-dominated or Pareto optimal solution. The collection of all Pareto optimal solutions is known as the Pareto optimal set or Pareto efficient set, instead, the corresponding objective vectors are described as the Pareto front or Trade-off surface. Unfortunately, the Pareto optimum concept typically does not give a single solution, but a set of possible solutions that cannot be used directly to find the final design solution by an analytic way. On the contrary, usually the decision about the 'best solution' to be adopted is formulated by so-called (human) decision maker (DM). On the other hand, several preference-based methods exist in literature. A more general classification of the preference-based method is considered when the preference information is used to influence the search (Kaufmann and San Francisco, 2000). Thus in a priori methods, DM's preferences are incorporated before the search begins. Therefore, based on the DM's preferences, it is possible to avoid producing the whole Pareto optimal set. In progressive methods, the DM's preferences are incorporated during the search: this scheme offers the advantage of driving the search process, but the DM may be unsure of his or her

DOI: 10.1002/tal

preferences at the beginning of the procedure and may be informed and influenced by information that becomes available during the search.

A last class of methods is a posteriori: in this case, the optimiser carries out the Pareto optimal set, and the DM chooses a solution ('searches first and decides later'). Many researchers view this last category as standard, so that in the greater part of the circumstances, a MOOP is considered resolved once that all Pareto optimal solutions are recognized.

In the category of a posteriori approaches, several methods are available in literature to treat multi-objective optimization problems using conventional single objective algorithms. The so-called ε-constraint method, due to its simplicity, is one of the most used techniques. This method is based on minimizing a single OF and considering the other objectives as constraints bound by some admissible levels ε. Another way to treat multi-objectives optimization by a standard SOP is by weighting the different OFs by normalized coefficients.

Moreover, it has been stated that this algorithm may find weakly non-dominated solutions, so that the more common way to approach MOOP is by using different Evolutionary Algorithms. Adopted algorithms are the Multiple Objective Genetic Algorithm (Fonsecam and Fleming, 1993) and the NSGA (Srinivas and Deb, 1994). In this work, the NSGA-II (Deb *et al*., 2000) is adopted in order to obtain the Pareto sets and the corresponding optimum DV values for different systems and input configurations. Particularly, the *Real Coded Genetic Algorithm* (Raghuwanshi and Kakde, 2004), *Binary Tournament Selection* (Blickle and Thiele, 1995), *Simulated Binary Crossover* (Deb and Agrawal, 1995) and *polynomial mutation* (Raghuwanshi and Kakde, 2004) are used (Appendix 2: Genetic operators adopted in NSGA-II).

5. CASE OF STUDY

In this section, a numerical analysis has been carried on a case study consisting in a 10-storey building equipped at the top floor with a TMD. Mechanical properties of the structure are given in Table 1.

Two different multi-objective problems are considered: problem a), in which the cost function is $I_{C_T^1}(\mathbf{b})$ and problem b), in which the cost function is $I_{C_T^2}(\mathbf{b})$. Different design variables are assumed: the first case includes only the frequency and damping of the TMD; the second one also the mass ratio μ.

To achieve the Pareto solutions, the NSGA-II is adopted (Deb *et al*., 2000). Setup parameters used in the analysis are given in Table 2. These have been obtained trial and error, where the choice derives from considerations about the equilibrium between computing cost and solution stability. The population size is 500, which is adequate to obtain a continuum Pareto front. The maximum iteration number is 100.

The proposed multi-objective optimization method was applied to an assigned structure and for a given stochastic model of the earthquake; therefore, the numerical results have the limitation of being valid for that earthquake and for that structure. However, because the proposed method is general, this can be applied to other cases of study, suitably modelling the structure to be analysed and the earthquake.

- ***Problem a)***

The first multi-objective optimization of a TMD concerns the search of the Pareto front and of the optimum DV $\mathbf{b} = (\omega_T, \xi_T)^T$ by assuming Eqs. (23) and (28) as OFs.

Seismic model parameters are given in Table 3.

Figure 2 shows that the variability of OF_1 and OF_2 is the space of the frequency ratio $\rho_\omega = \frac{\omega_T}{\omega_1}$ (i.e. the TMD frequency over the main system fundamental frequency) and the TMD damping ratio ξ_T. By comparing these surfaces, it is quite evident that they show an opposite behaviour: as OF_1 decreases until a minimum point (this corresponds to the best TMD performance), OF_2 monotonically increases. This consideration confirms the impossibility to achieve the multiple OF minimization in an absolute sense, both in terms of structural performance, minimizing the absolute acceleration, and of protection cost minimization.

Table 1. Main structure mechanical characteristics.

	Mode/level									
	1	2	3	4	5	6	7	8	9	10
T_i (s)	1.3444	0.5064	0.3127	0.2299	0.1855	0.1584	0.1396	0.1245	0.1113	0.0987
$k_i(Nm)$	4.5 10^8	4.1 10^8	3.8 10^8	3.5 10^8	3.2 10^8	2.8 10^8	2.5 10^8	2.2 10^8	1.8 10^8	1.5 10^8
$c_i(Nm/s)$	1.25 10^6	1.21 10^6	1.16 10^6	1.11 10^6	1.05 10^6	0.99 10^6	0.93 10^6	0.87 10^6	0.80 10^6	0.72 10^6
$m_i(kg)$	3.5 10^5	3.5 10^5	3.5 10^5	3.5 10^5	3.5 10^5	3.5 10^5	3.5 10^5	3.5 10^5	3.5 10^5	3.5 10^5

Table 2. Input data for GA.

Input data for GA	
Maximum generation	500
Population size	100
Crossover probability	0.9
Mutation probability	0.1

Table 3. Input data, problem a).

ω_f	ξ_f	S_0	μ	α_C
$9\pi rad$/s	0.4	300 cm^2/s^3	2 %	50

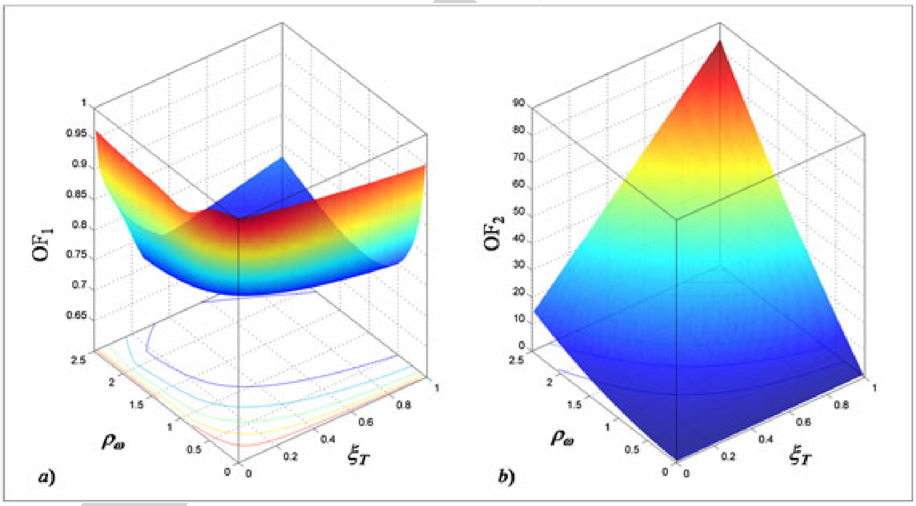

Figure 2. OF_1 (a) and OF_2 (b) versus ξ_T and $\rho\omega$.

In Figure 3, the optimum design variables and the contour lines of OF surfaces are plotted overlapped, in order to more clearly observe the location of Pareto solutions with respect to the single optimization one.

Figure 4 shows the Pareto front (b) and the corresponding optimum DV components $\xi_T^{opt}\rho_\omega^{opt}$ (a).

In particular, Figure 4b points out an asymptotic limit, which simultaneously corresponds to the highest effectiveness of the TMD and the highest cost $I_{C_T^1}^{OPT}$. This means that the advantage in terms of increase of TMD performance is negligible in comparison with the cost growing.

By analysing the Pareto front and the optimum design variables, two different strategies can be distinguished with the aim to optimize the TMD.

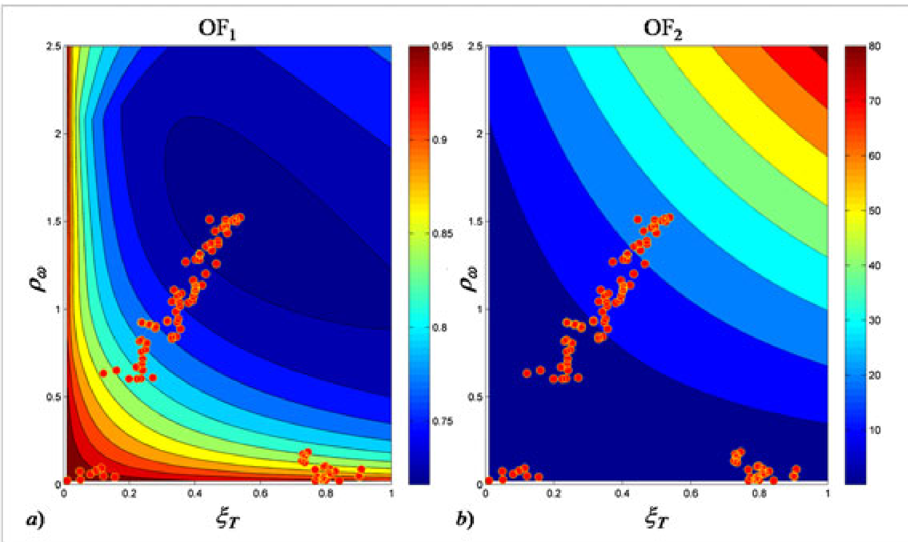

Figure 3. OF_1 (a) and OF_2 (b) and Pareto solutions plotted in the space state domain.

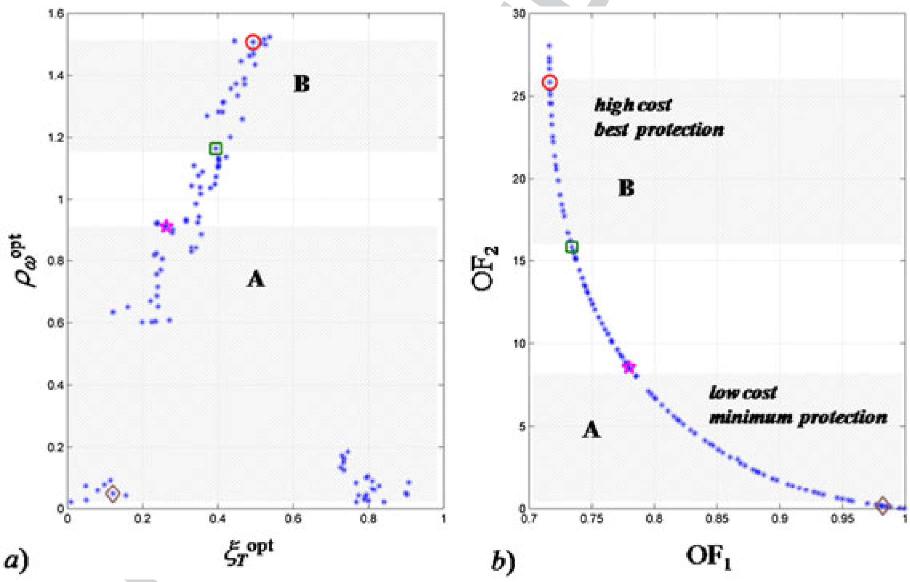

Figure 4. Optimal tuned mass damper parameters (a) and Pareto front (b).

- ***Strategy 1***: corresponds to the Pareto front region between the pink star and the brown rhombus (region A) concerning low-medium TMD costs. In this region, the TMD increases the vibration protection efficiency essentially working by means of the tuned frequency. Starting from a low TMD cost (the lowest protection level represented by the rhombus symbol) and moving towards higher costs, the optimum TMD frequency ratio increases obtaining higher protection levels, whereas the TMD optimal damping ratio is almost constant and equal to its minimum value, as clearly indicated by the location of the optimal solutions in Figure 4 (a). Besides in this region, it is worth to note that this important protection increase, due to the increase of the optimum frequency ratio, does not lead to a relevant increase of cost. This is a direct effect of the circumstance that increasing only the TMD frequency is cheaper than increasing the damping, as a consequence of the definition of the factor α_C in Eq. (26), which is assumed to be greater than one.

DOI: 10.1002/tal

- ***Strategy 2***: in *region B* (the front portion between the green square and the red circle) characterized by high-medium costs, the reduction of vibration levels in the main structure can be achieved by tuning the TMD frequency to the main structure one (as indicated in Figure 4 (a), ρ is about 0.9 at the level of the pink star). The tendency demonstrates that the best structural protection performance (indicated by the Red Circle) can be achieved by applying tuned masses with high tuned damping and frequency larger than the system one. This gain in terms of protection efficiency is paid by a very high increasing of cost. In fact, it is quite clear that the most significant reductions of vibration effects on the main structure are obtained working mainly on the TMD damping that essentially increases the energy dissipation. In this case, a cost increase takes place. It is also important to remark that, in this situation, with an increase of the optimal TMD damping ratio, only a moderate increasing of TMD efficiency is achieved. As a consequence, this approach cannot be considered economically convenient because the cost increase reaches a percentage equal to about 70% whereas the efficiency increase does not exceed the 7%. Then, starting from ρ equal to about one, the increasing of cost prevails on the protection efficiency improvement.

The two opposite above described strategies are synthesized in Table 4.

In the following figures, the Pareto front sensitivity versus different parameters is also shown. More precisely, the analysis is developed by varying the mass ratio μ (Figure 5), the cost parameter α_C (Figure 6), the structure–earthquake frequency ratio ψ_ω (Figure 7) and the structural damping coefficient ξ_i (Figure 8). In these figures, all constant parameters are assumed to be the same of the previous analysis.

Table 4. Main trend of extreme data.

Front portion	Kind of strategy	Tuned efficiency
A	Strategy 1	High-protection performance increasing in comparison to cost increasing
	Based on increasing of tuning optimum frequency	Strategy economically convenient
B	Strategy 2	High costs increasing in comparison with protection increasing
	Based on increasing of tuning optimum damping	Strategy economically not convenient

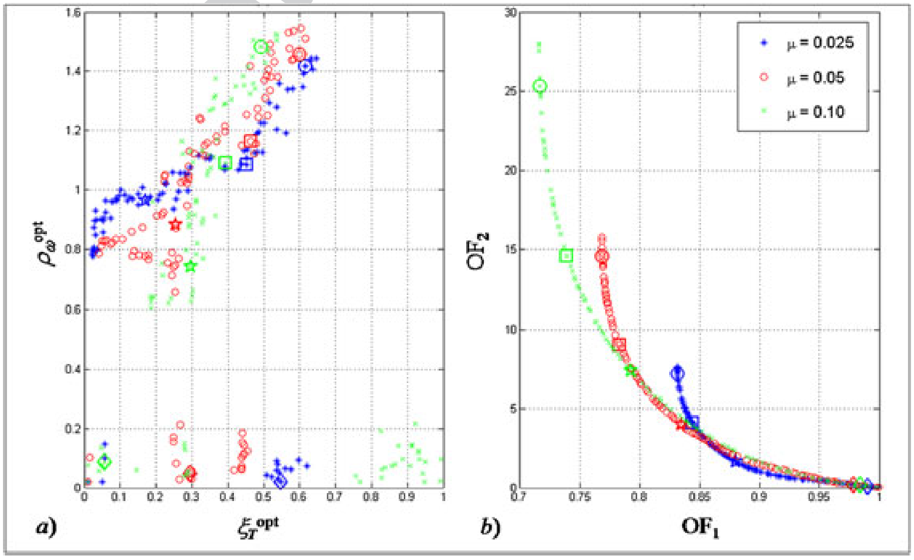

Figure 5. Optimal tuned mass damper parameters (a) and Pareto front (b) for different values of the mass ratio μ (case a).

DOI: 10.1002/tal

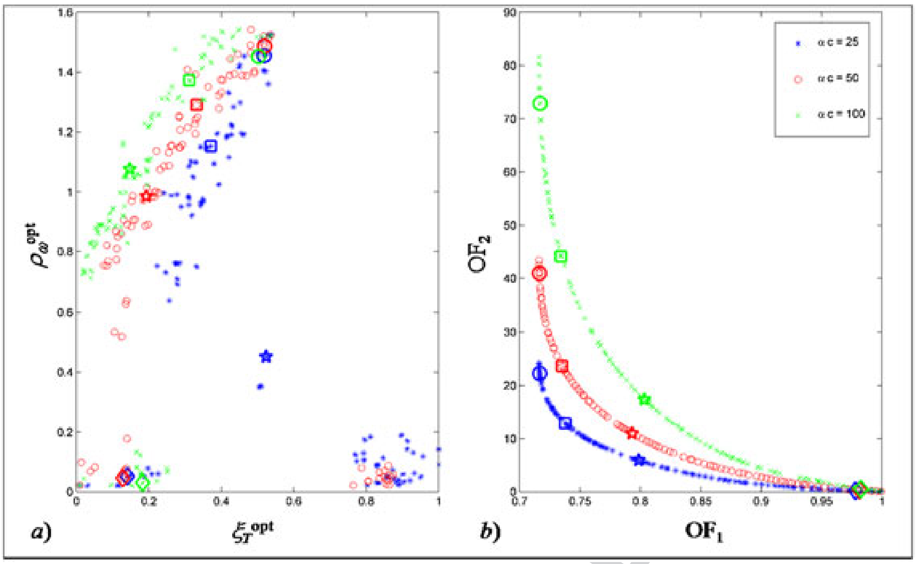

Figure 6. Optimal tuned mass damper parameters (a) and Pareto front (b) for different values of the cost factor ψ_T.

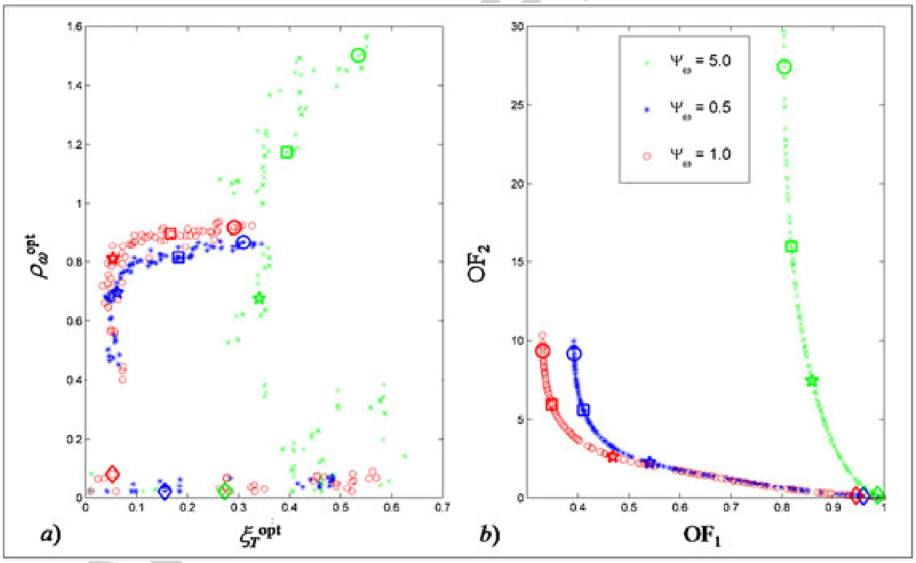

Figure 7. Optimal tuned mass damper parameters (a) and Pareto front (b) for different values of the structure–earthquake frequency ratio ψ_ω.

In Figure 5, the Pareto fronts obtained by assuming different mass ratios are depicted. The values adopted for this parameter are 2%, 6% and 10%. It is clear that by varying the value of the mass ratio, significant differences occur in the Pareto optimal set. If this parameter increases, as well known, also the protection efficiency increases. At the same time, the TMD cost increases, this latter being indirectly correlated to the mass ratio by the TMD frequency. So, if a protection level is obtainable with different mass ratio values, the cheapest solution is achieved with the minimum μ. Nevertheless, if a very large reduction of system response is requested, it is necessary to adopt larger values of μ.

In the DV space, it can be also noted that in the region of low protection level-low cost, it is not possible to identify a regular behaviour of the variation of DVs components as μ varies.

Figure 6 shows the Pareto fronts obtained by varying the *cost factor* parameter α_C. It is clear that this variation does not modify the asymptotic protection level obtainable by adopting the TMD strategy,

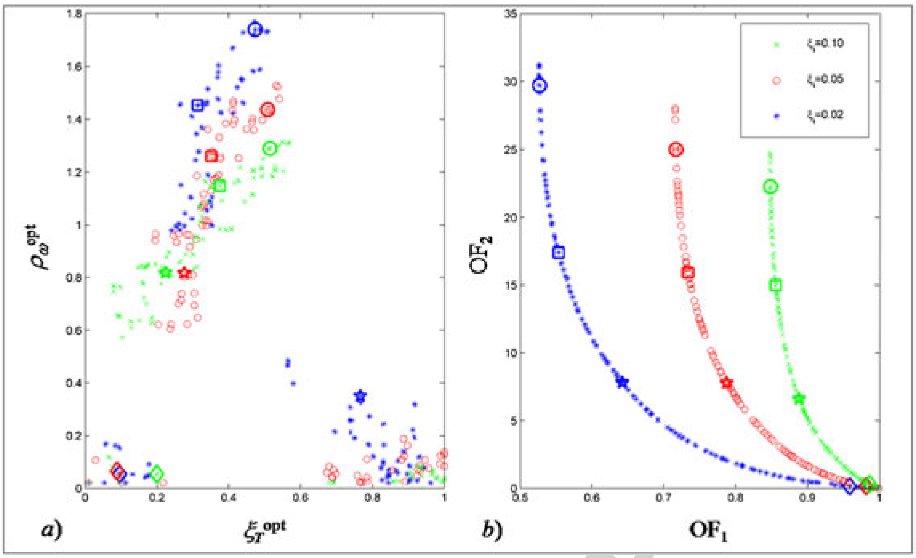

Figure 8. Optimal tuned mass damper parameters (a) and Pareto front (b) for different values of the structural damping coefficient ξ_i.

whereas total cost varies. In fact, the maximum effectiveness of TMD is only obtainable by increasing the damping ratio, as shown in Figure 4.

Similarly for low protection level, the Pareto set does not show significant modifications as α_C varies, since the optimal solutions essentially depend on the TMD frequency.

In Figure 7, the results of the sensitivity analysis are shown in function of the structure–earthquake frequency ratio, defined as the fundamental frequency of the main system ω_1 over the filter frequency ω_f:

$$\psi_\omega = \frac{\omega_1}{\omega_f} \tag{47}$$

This parameter is assumed equal to 0.5, 1.0 and 5.0. By observing these plots, it can be deduced that the change of this parameter induces serious modifications in the Pareto front, sensibly affecting the maximum efficiency obtainable by means of the TMD strategy. More in detail, results show that

- for $\psi_\omega \leq 1$, the optimal points in the DV space domain are well distributed, assuming a characteristic ‘handle’ shape. This particular shape suggests that, initially, the TMD mainly works by increasing the frequency and successively (when the points turn on the right in Figure 7a) by increasing the damping. The gain in terms of performance is very high, and a very little growing of cost takes place, as demonstrated by the distribution of the Pareto fronts in Figure 7b.
- for $\psi_\omega > 1$, the optimal points in Figure 7a appear very scattered but distributed along a straight line. The corresponding Pareto front shows a very low reduction of the vibration level compared with an immoderate increasing of cost.

These observations allow to state that the best protection performance is achieved when the main system frequency is in the sensitive-acceleration region (at left of the resonance condition) or in the resonance region.

Finally, in Figure 8, the results of a sensitivity analysis carried out by varying the structural damping are presented. As well known, the variation of ξ_i induces a relevant change in the maximum protection level achieved by the optimum solution; the TMD strategy becomes more efficient for structures with a low damping. Also in this situation, the differences are more evident in the left region of the Pareto set and tend to vanish in the right side of it.

- ***Problem b)***

In the following examples, the Pareto fronts are obtained by assuming also the mass ratio as a design variable. Therefore, DV is $\mathbf{b} = (\omega_T, \xi_T, \mu)^T$, and the OFs are those reported in Eqs. (23) and (33).

DOI: 10.1002/tal

Figure 9 shows the corresponding Pareto front and Figure 10 the space of the optimum DV components. Input data are given in Table 5.

It can be noted that the Pareto set shape is strongly influenced by the strategy adopted to define the DV optimum values. First of all, if also the mass ratio is optimized, a better performance can be achieved. Starting from the points on the left of Figure 9b and observing Figure 10, it emerges that the increase of the TMD efficiency is obtained before by the increase of only ρ_{ω}^{opt}, then by a moderate increase of ξ_T^{opt} and finally by the increase of μ_T^{opt}. Besides, some characteristics in Pareto set shown in Figure 9a should be pointed out. Firstly, a quite short portion recognizable in the upper-extreme left

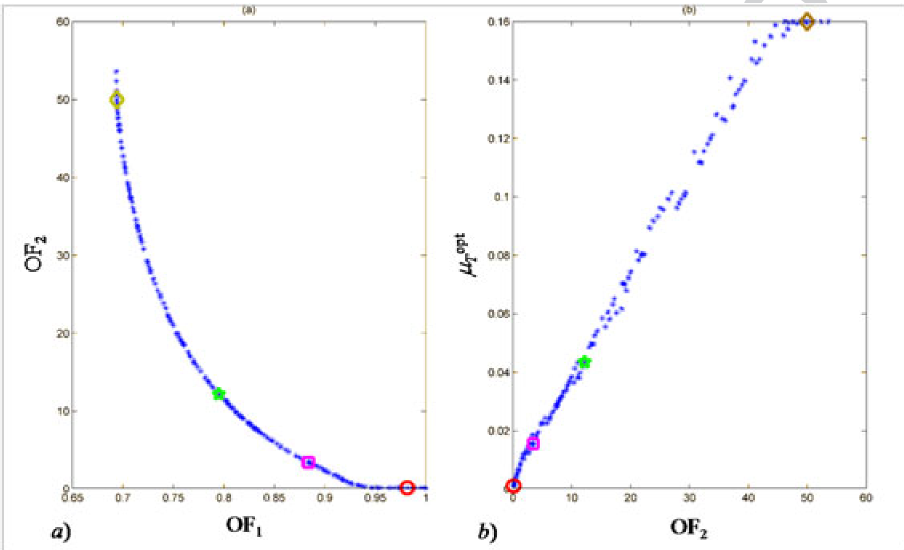

Figure 9. Pareto front (a) and optimal tuned mass damper parameters (b) by assuming also the mass ratio as design variable (case b).

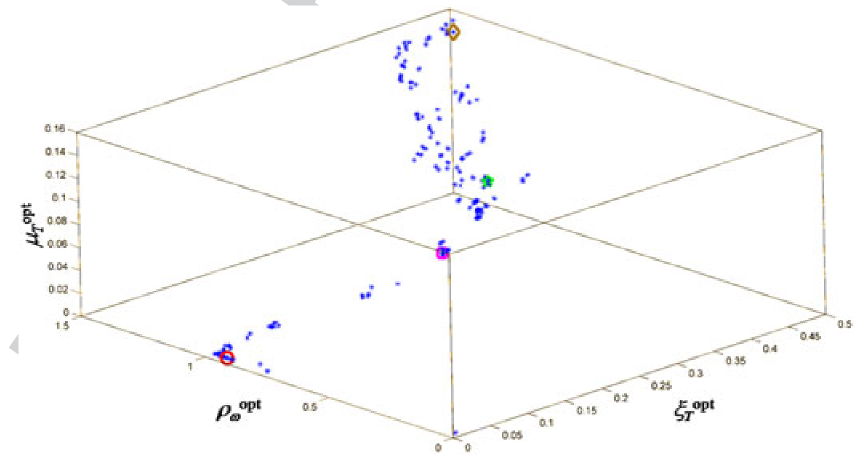

Figure 10. Space of design vector components by assuming also the mass ratio as design variable (case b).

Table 5. Input data in problem b).

Input data for secondary and primary systems				
ω_f	ξ_f	S_0	θ_T	ψ_T
$9\pi rad/s$	0.4	100 cm^2/s^3	0.5	50

region of the front corresponds to a moderate increase of TMD cost and structural efficiency. After that, moving on the right of the Pareto set, a portion with a more significant increase of structural efficiency takes place, also with a quite linear low. Finally the lower-extreme right of the Pareto set is a quite linear segment, due to a reduction of the set inclination compared with the previous one. This portion is characterized by a worse performance.

CONCLUSIONS

In this work, a multi-objective optimum criterion for TDM device has been proposed, considering both economic and performance indices. The ratio between the protected and the unprotected system absolute accelerations has been considered as a first OF. A further objective, related to the cost of the protection system, has been further considered. These two OFs are antithetic, and therefore the NSGA-II has been performed to achieve optimum Pareto solutions.

Pareto fronts show that two different strategies can be distinguished with the aim to optimize the TMD.

- A first strategy based on the increase of TMD frequency. This strategy corresponds to a high TMD performance in comparison with the cost, and therefore this strategy is economically convenient;
- A second strategy based on increasing the TMD damping. In this case, the increase of the costs is high in comparison with the protection increase. This strategy is economically not convenient.

Moreover, it has been pointed out how some parameters as the input spectral content, the main structural frequency and the damping or tuned mass ratio can induce strong variations on the Pareto optimal front and on the best TMD parameters.

More in detail, varying the mass ratio, significant differences occur in the Pareto optimal set. If this parameter increases, also the protection efficiency increases but at the same time, the TMD cost increases, this latter being indirectly correlated to the mass ratio by the TMD frequency. The sensitivity analysis by varying the earthquake frequency content has showed that the best protection performance is achieved when the main system frequency is in the sensitive-acceleration region or in the resonance region. Finally, the variation of structural damping ratio induces a relevant change in the maximum protection level achieved by the optimum solution, and the TMD strategy becomes more efficient for structures with a low damping.

The novelty of the proposed method is in using a multi-dimensional criterion for the design of TMD. A possible future development of this research could consist in considering the uncertainty in structural parameters and thus analyse their influence on the TMD optimum design.

LIST OF NOTATIONS

The following symbols are used in the paper:

$\ddot{X}_b$	acceleration that excites the system at the base
$\mathbf{\Omega_b}$	admissible domain of the design parameters
ω_f	filter frequency
ξ_f	filter damping
$\mathbf{b}$	design vector
$Y_f(t)$	displacement process of the filter
ψ_ω	frequency ratio
ω_s	main structural circular frequency
ξ_s	main structural damping
B	null matrix of the Lyapunov equation for the protected structure
S_0	power spectral density intensity of white noise excitation at the bed rock
μ	ratio between the tuned and main masses
$\ddot{X}_f$	relative acceleration process of the filter
$.X_f$	velocity process of the filter

DOI: 10.1002/tal

X_f displacement process of the filter
$\ddot{\mathbf{X}}(t)$ acceleration vector
$\mathbf{X}(t)$ displacement vector
$\mathbf{R}_{ZZ}$ state space covariance matrix of the protected structure
$\mathbf{Z}$ state space vector of the protected structure
$\sigma_{\ddot{y}_N}$ standard deviation of the top floor displacement of the protected structure
$\sigma^0{}_{\ddot{y}_N}$ standard deviation of the top floor displacement of the unprotected structure
A state matrix of the structure
$w(t)$ stationary Gaussian zero mean white noise process
ω_T tuned mass damper circular frequency
ξ_T tuned mass damper damping
C damping system matrix
K stiffness system matrix
M mass system matrix
OF_1 §performance index
OF_2 cost function
C_1^T tuned mass damper cost function
C_2^T tuned mass damper cost function
α_C cost parameter
ϑ_T cost parameter

APPENDIX 1

THE DIAGONAL MATRIX **M** OF MASSES IS

$$M = \begin{bmatrix} m_1 & 0 & \cdots & \cdots & 0 \\ 0 & m_2 & \ddots & \ddots & \vdots \\ \vdots & \ddots & \ddots & \ddots & \vdots \\ \vdots & \ddots & \ddots & m_n & 0 \\ 0 & \cdots & \cdots & 0 & m_T \end{bmatrix}$$

THE THREE-DIAGONAL SYMMETRIC MATRIX **K** OF STIFFNESS IS

$$\mathbf{K} = \begin{bmatrix} k_1 + k_2 & -k_2 & \cdots & \cdots & 0 \\ -k_2 & k_2 + k_3 & \ddots & \ddots & \vdots \\ \vdots & -k_3 & \ddots & -k_n & \vdots \\ \vdots & \ddots & -k_n & k_n + k_T & -k_T \\ 0 & \cdots & \cdots & -k_T & k_T \end{bmatrix}$$

THE TWO (N + 1)(N + 1) SUBMATRICES $\mathbf{M}^{-1}\mathbf{C}$ AND $\mathbf{M}^{-1}\mathbf{K}$ ARE, RESPECTIVELY

$$\mathbf{M}^{-1}\mathbf{K} = \begin{bmatrix} \beta_1^2 + \mu_1\beta_2^2 & -\mu_1\beta_2^2 & 0 & .. & 0 \\ -\beta_2^2 & \beta_2^2 + \mu_2\beta_3^2 & -\mu_2\beta_3^2 & .. & \vdots \\ 0 & -\beta_3^2 & \cdots & .. & 0 \\ \vdots & .. & .. & \beta_{n-1}^2 + \mu_{n-1}\beta_n^2 & -\beta_T^2 \\ 0 & .. & 0 & -\beta_T^2 & \beta_T^2 \end{bmatrix}$$

DOI: 10.1002/tal

$$\mathbf{M}^{-1}\mathbf{C}=\begin{bmatrix} 2\psi_1\beta_1+\mu_1 2\psi_2\beta_2 & -\mu_1 2\psi_2\beta_2 & 0 & .. & 0 \\ -2\psi_2\beta_2 & 2\psi_2\beta_2+\mu_2 2\psi_3\beta_3 & -\mu_2 2\psi_3\beta_3 & .. & \vdots \\ 0 & -2\psi_3\beta_3 & \dots & .. & 0 \\ \vdots & .. & .. & 2\psi_{n-1}\beta_{n-1}+\mu_{n-1}2\psi_n\beta_n & -2\psi_T\beta_T \\ 0 & .. & 0 & -2\psi_T\beta_T & 2\psi_T\beta_T \end{bmatrix}$$

APPENDIX 2
SIMULATED BINARY CROSSOVER

In Simulated Binary Crossover, the probability distribution used to create a child solution is derived to have a similar search power as that in a single-point crossover in binary-coded genetic algorithms and is given as follows:

$$P(\beta)=\begin{cases} \frac{1}{2}(\eta_c+1)\beta_k^{\eta_c} & \text{if } 0\leq\beta\leq 1 \\ \frac{1}{2}(\eta_c+1)\frac{1}{\beta_k^{\eta_c+2}} & \text{otherwise} \end{cases} \tag{A2.1}$$

where η_c is the distribution index for crossover operator. Therefore, first, a random number $u_k \in [0,1]$ is generated, and using expression (A2.1), β_k is calculated with this formulation:

$$\beta_k=\begin{cases} (2u_k)^{\frac{1}{\eta_c+1}} & \text{if } u_k\leq 0.5 \\ \frac{1}{[2(1-u_k)]^{\frac{1}{\eta_c+1}}} & \text{otherwise} \end{cases} \tag{A2.2}$$

After obtaining β from (A2.2), the children solutions are calculated as follows:

$$c_{1,k}=\frac{1}{2}\left[(1-\beta_k)p_{1,k}+(1+\beta_k)p_{2,k}\right] \tag{A2.3}$$

$$c_{2,k}=\frac{1}{2}\left[(1+\beta_k)p_{1,k}+(1-\beta_k)p_{2,k}\right] \tag{A2.4}$$

In (A2.3) and (A2.4), $c_{i,k}$ is the i^{th} child with k^{th} component and $p_{i,k}$ is the selected parent.

POLYNOMIAL MUTATION

Polynomial mutation is performed on one string as follows:

$$c_k=p_k+\left(p_k^u-p_k^l\right)\delta_k \tag{A2.5}$$

In (A2.5), p_k is the parent with p_k^u and p_k^l are the upper bound and lower bound on the parent component, c_k is the child. Mutation operator is based on δ_k which is calculated from a polynomial distribution. First, a random number $r_k \in [0,1]$ is generated, and δ_k is calculated with this formulation:

$$\delta_k=\begin{cases} (2r_k)^{\frac{1}{\eta_m+1}}\text{-}1 & \text{if } r_k<0.5 \\ 1\text{-}[2(1-r_k)]^{\frac{1}{\eta_m+1}} & \text{if } r_k\geq 0.5 \end{cases} \tag{A2.6}$$

In (A2.6), η_m is the mutation distribution index.

DOI: 10.1002/tal

REFERENCES

Blickle T, Thiele L. 1995. A mathematical analysis of tournament selection. Genetic Algorithms: Proceedings of the 6th International Conference (ICGA95), Eschelman L, ed..

M Kaufmann, San Francisco, CA, pp 9–16 Coello Coello CA. 2000. Handling preferences in evolutionary multiobjective optimization: a survey. In: IEEE Neural Networks Council (ed) Proceedings of the 2000 Congress on Evolutionary Computation (CEC 2000) vol 1. IEEE Service Center, Piscataway, New Jersey: 30–37.

Crandall SH, Mark WD. 1973. Random Vibration in Mechanical System. Academic.

Deb K, Agrawal RB. 1995. Simulated binary crossover for continuous search space. *Complex Syst* **9**: 115–148.

Deb K, Agrawal S, Pratap A, Meyarivan T. 2000. A Fast Elitism Multi-objective Genetic Algorithm: NSGA-II". Proceedings of Parallel Problem Solving from Nature. Springer; 849–858.

Fiore A, Monaco P. 2010. Earthquake-induced pounding between the main buildings of the 'Quinto Orazio Flacco' school. *Earthquakes and Structures* **1**(4): 371–390.

Fiore A, Monaco P. 2011. 'Analisi della vulnerabilità sismica del Liceo "Quinto Orazio Flacco" in Bari' [Analysis of the seismic vulnerability of the 'Quinto Orazio Flacco' school in Bari (Italy)]. *Ingegneria Sismica* **28**(1): 43–62.

Fiore A, Berardi L, Marano GC. 2012. Predicting torsional strength of RC beams by using evolutionary polynomial regression. *Advances in Software Engineering* **47**(1): 178–187.

Fiore A, Marano GC, Monaco P. 2013. Earthquake-induced lateral-torsional pounding between two equal height multi-storey buildings under multiple bi-directional ground motions. *Advances in Structural Engineering* **16**(5): 845–865.

Fiore A, Quaranta G, Marano GC, Monti G. 2015. Evolutionary polynomial regression–based statistical determination of the shear capacity equation for reinforced concrete beams without stirrups. *Journal of Computing in Civil Engineering, ASCE*. DOI:10.1061/(ASCE)CP.1943-5487.0000450.

Fonsecam CM, Fleming PJ. 1993. Genetic algorithms for multiobjective optimization: formulation, discussion and generalization. Genetic Algorithms: Proceedings of the 5th International Conference, Forrest S, ed. July.. Morgan Kaufmann.

San Mateo CA, Fu TS, Johnson EA. 2011. Distributed mass damper system for integrating structural and environmental control in buildings. *Journal of Engineering Mechanics* **137**(3): 205–213.

Greco R, Marano GC. 2015. Optimum design of viscous dissipative links in wall-frame. *Structural Design of Tall and Special Buildings*. DOI:10.1002/tal.1265.

Greco R, Marano GC. 2013. Optimum design of tuned mass dampers by displacement and energy perspectives. *Soil Dynamics and Earthquake Engineering* **49**: 243–253.

Greco R, Lucchini A, Marano GC. 2014a. Robust design of tuned mass dampers installed on multi degree of freedom structures subjected to seismic action. *Engineering Optimization* **47**(8): 1009–1030.

Greco R, Fiore A, Marano GC. 2014b. The role of modulation function in nonstationary stochastic earthquake model. *Journal of Earthquake and Tsunami* **8**(5 1450015 (28 pages)).

Hoang N, Warnitchai P. 2005. Design of multiple tuned mass dampers by using a numerical optimizer. *Earthquake Engineering and Structural Dynamics* **34**: 125–144.

Hoang N, Fujino Y, Warnitchai P. 2008. Optimal tuned mass damper for seismic applications and practical design formulas. *Engineering Structures* **30**(3): 707–715.

Quaranta G, Fiore A, Marano GC. 2014. Optimum design of prestressed concrete beams using constrained differential evolution algorithm. *Structural and Multidisciplinary Optimization* **49**(3): 441–453.

Jennings PC, Housener GW, Tsai NC. 1968. Simulated earthquake motions for design purpose. *Proceedings of 4th World Conference Earthquake Engineering*. A-1:145–60.

A Kareem and S Kline, Performance of multiple mass dampers under random loading 1995. *Journal of Structural Engineering*, **121**(2), 348–361, .

Krenk S, Høgsberg J. 2008. Tuned mass absorbers on damped structures under random load. *Probabilsitic Engineering Mechanics* **23**: 408–415.

Li H, Ni X. 2007. Optimization of non-uniformly distributed multiple tuned mass damper. *Journal of Sound and Vibration* **308**: 80–97.

Lucchini A, Greco R, Marano GC, Monti G. 2014. Robust design of tuned mass damper systems for seismic protection of multistory buildings. *Journal of Structural Engineering* **140**(8 A4014009).

Marano GC, Greco R. 2009. Robust optimum design of tuned mass dampers for high-rise buildings under moderate earthquakes. *Structural Design of Tall and Special Buildings* **18**(8): 823–838.

Marano GC, Greco R, Chiaia B. 2010. A comparison between different optimization criteria for tuned mass dampers design. *Journal of Sound and Vibration* **329**(23): 4880–4890.

Marano, GC, Greco, R 2011. Optimization criteria for tuned mass dampers for structural vibration control under stochastic excitation. *Journal of Vibration and Control*, **17**(5), pp. 679–688,.

Marano GC, Greco R, Quaranta G, Fiore A, Avakian J, Cascella D. 2013. Parametric identification of nonlinear devices for seismic protection using soft computing techniques. *Advanced Materials Research* **639-640**(1): 118–129.

Marano GC, Acciani G, Fiore A, Abrescia A. 2015. Integration algorithm for covariance non-stationary dynamic analysis of SDOF systems using equivalent stochastic linearization. *International Journal of Structural Stability and Dynamics* **15** (2 1450044 (17 pages)).

Mohebbi M, Shakeri K, Ghanbarpour Y, Majzub H. 2013. Designing optimal multiple tuned mass dampers using genetic algorithms (GAs) for mitigating the seismic response of structures. *Journal of Vibration and Control* **19**(4): 605–625.

Nigam NC. 1972. Structural optimization in random vibration environment. *AIAA Journal* **10**: 551–553.

Ormondroyd J, Den Hartog JP. 1928. The theory of dynamic vibration absorber. *Journal of Applied Mechanics Trans. ASME* **50** (7): 9–22.

Raghuwanshi MM, Kakde OG. 2004. Survey on multiobjective evolutionary and real coded genetic algorithms. Proceedings of the 8th Asia Pacific symposium on intelligent and evolutionary systems: 150–161.

Rana R, Soong TT. 1998. Parametric study and simplified design of tuned mass dampers. *Engineering Structures* **20**(3): 193–204.

Rundinger F. 2006. Otimal vibration absorber with nonlinear viscous power law damping and white noise excitation, ASCE. *Journal of Engineering Mechanics* **132**: 46–53.

Sadek F, Mohraz B, Taylor AW, Chung RM. 1997. A method of estimating the parameters of tuned mass dampers for seismic applications. *Earthquake Engineering and Structural Dynamics* **26**(6): 617–635.

Srinivas N, Deb K. 1994. Multi-objective optimization using nondominated sorting in genetic algorithms. *Journal of Evolutionary Computation* **2**(3): 221–248.

Villaverde R. 1985. Reduction in seismic response with heavily-damped vibration absorbers. *Earthquake Engineering and Structural Dynamics* **13**(1): 33–42.

Villaverde R, Koyama LA. 1993. Damped resonant appendages to increase inherent damping in buildings. *Earthquake Engineering and Structural Dynamics* **22**(6): 491–507.

Zitzler E, Thiele L. 1999. Multi-objective evolutionary algorithms: a comparative case study and the strength Pareto approach. *IEEE Transactions on Evolutionary Computation* **3**: 257–271.

Zuo L, Nayfeh SA. 2005. Optimization of the individual stiffness and damping parameters in multiple-tuned-mass-damper system. *Journal of Vibration and Acoustics (ASME)* **127**(1): 77–83.

Zuo L, Nayfeh S. 2006. The two degree of freedom tuned mass damper for suppression of single mode vibration under random and harmonic excitation. *Transactions of the ASME* **128**(Feb): 56–65.